Mechanisms underlying the protective effect of tannic acid against arsenic trioxide-induced cardiotoxicity in rats: Potential involvement of mitochondrial apoptosis

YUCONG XUE[1*], MENGYING LI[1*], YURUN XUE[1], WEIYUE JIN[1], XUE HAN[1,2],
JIANPING ZHANG[3], XI CHU[4], ZILIANG LI[3] and LI CHU[1,5]

[1]School of Pharmacy, Hebei University of Chinese Medicine, Shijiazhuang, Hebei 050200;
[2]Hebei Higher Education Institute Applied Technology Research Center on TCM Formula Preparation,
Shijiazhuang, Hebei 050091; [3]School of Basic Medicine, Hebei University of Chinese Medicine,
Shijiazhuang, Hebei 050200; [4]The Fourth Hospital of Hebei Medical University, Shijiazhuang, Hebei 050011;
[5]Hebei Key Laboratory of Chinese Medicine Research on Cardio-cerebrovascular Disease,
Shijiazhuang, Hebei 050200, P.R. China

Abstract. Arsenic trioxide (ATO) is a frontline chemotherapy drug used in the therapy of acute promyelocytic leukemia. However, the clinical use of ATO is hindered by its cardiotoxicity. The present study aimed to observe the potential effects and underlying mechanisms of tannic acid (TA) against ATO-induced cardiotoxicity. Male rats were intraperitoneally injected with ATO (5 mg/kg/day) to induce cardiotoxicity. TA (20 and 40 mg/kg/day) was administered to evaluate its cardioprotective efficacy against ATO-induced heart injury in rats. Administration of ATO resulted in pathological damage in the heart and increased oxidative stress as well as levels of serum cardiac biomarkers creatine kinase and lactate dehydrogenase and the inflammatory marker NF-κB (p65). Conversely, TA markedly reversed this phenomenon. Additionally, TA treatment caused a notable decrease in the expression levels of cleaved caspase-3/caspase-3, Bax, p53 and Bad, while increasing Bcl-2 expression levels. Notably, the application of TA decreased the expression levels of cytochrome c, second mitochondria-derived activator of caspases and high-temperature requirement A2, which are apoptosis mitochondrial-associated proteins. The present findings indicated that TA protected against ATO-induced cardiotoxicity, which may be associated with oxidative stress, inflammation and mitochondrial apoptosis.

Introduction

Arsenic, a naturally prevalent element, is found in the environment and certain foods. Arsenic has two forms in the environment: Organic and inorganic. Inorganic arsenic has two valences: Arsenite (III) and arsenate (V) (1). Generally, inorganic arsenic is more toxic than organic arsenic, and trivalent arsenic is more toxic than pentavalent arsenic (2). Arsenic trioxide (ATO) is the primary effective ingredient of white arsenic, which is inorganic arsenic. It has been used in the therapy of acute promyelocytic leukemia since the early 1990s. ATO is a safe and effective anticancer drug and is not prone to drug resistance (3). Researchers have attempted to use ATO in the treatment of other types of tumor: ATO has also been reported to achieve a favorable therapeutic effect in the treatment of malignant tumors such as lymphoma, gastric (4), esophageal (5), liver and lung cancer, neuroblastoma (6) and breast cancer (7).

However, in the treatment of solid tumors, high concentrations of ATO can cause serious side effects, such as cardiotoxicity (8), hepatotoxicity (9), fluid retention (10), alimentary symptoms (11) and rash (12). ATO induces serious cardiotoxicity and potential cardiovascular side effects, including sudden death due to acute toxic myocardial damage (13,14). ATO also has a toxic effect on the liver, kidney and nervous system (15-17). These factors limit the clinical application of ATO. Potential mechanisms of ATO-induced cardiotoxicity include oxidative stress, mitochondrial DNA injury, apoptosis and functional disruption of ion channels (18). Several studies have indicated that mitochondrial damage, caspase activation and

Correspondence to: Professor Ziliang Li, School of Basic Medicine, Hebei University of Chinese Medicine, 6 Xingyuan Road, Shijiazhuang, Hebei 050200, P.R. China
E-mail: liziliang321@126.com

Professor Li Chu, School of Pharmacy, Hebei University of Chinese Medicine, 6 Xingyuan Road, Shijiazhuang, Hebei 050200, P.R. China
E-mail: chuli0614@126.com

*Contributed equally

p53 signaling are the pathways underlying arsenic-induced apoptosis (1,18).

Mitochondria, intracellular double membrane organelles, are considered the 'power plant' of eukaryotic cells (19). Mitochondria are the primary site of intracellular oxidative phosphorylation and synthesis of adenosine triphosphate, which provides energy for cell activity (20). Mitochondria also participate in cell signaling, differentiation, proliferation and apoptosis (21). The heart, the most energy consuming organ, has the highest content of mitochondria of all types of tissue (22). The heart requires efficient oxidative metabolism and derives almost all of its energy from mitochondrial oxidative phosphorylation (23). Therefore, mitochondria are important for myocardial development as well as healthy function. Beyond their role as a cellular powerhouse, mitochondria produce reactive oxygen species (ROS) (24), which lead to oxidative injury and regulate cardiomyocyte apoptosis. Hence, mitochondrial dysfunction and ROS production are considered key factors in cardiac disease. Creatine kinase (CK) and lactate dehydrogenase (LDH) are vital biomarkers for the diagnosis of myocardial injury (25). Studies have shown that ATO increases LDH content and consequently results in cardiomyocyte necrosis (26,27).

There are two major antioxidant systems in the body: The enzyme antioxidant system [involving superoxide dismutase (SOD) and catalase (CAT)] and the non-enzyme antioxidant system (involving vitamins C and E, glutathione, carotenoid, copper and zinc) (28). When oxidative stress occurs, these two systems are out of balance, which leads to tissue damage (29). Studies have shown that excessive ROS during ATO treatment leads to destruction in the endogenous antioxidant system (30,31). In addition, studies have suggested that high doses of ATO can cause oxidative stress, increased ROS and inhibit enzyme and mitochondrial activity (32,33). Mitochondrial impairment leads to the release of mitochondrial-associated proteins cytochrome *c*, second mitochondria-derived activator of caspases (Smac) and high-temperature requirement A2 (HtrA2); the release of cytochrome *c* can activate caspase-3 (34). Moreover, the Bcl-2 family, which serves a crucial role in the regulation of cardiomyocyte apoptosis, is a primary regulator of cytochrome *c* release and caspase-3 activation (34). Arsenic exposure increases the levels of pro-apoptotic proteins Bax (35) and Bad (36) and decreases the expression levels of anti-apoptotic protein Bcl-2 (37). Furthermore, one study reported that arsenic exposure activates phosphorylation of the NF-κB pathway (36). The NF-κB pathway participates in the inflammatory response, which results in apoptosis (38). Thus, we hypothesized that the potential mechanism of ATO-induced cardiotoxicity may be associated with oxidative stress, inflammation and mitochondrial apoptosis.

Tannic acid (TA) is found in plants and foods, such as apples, pears, beans, tea and red wine. TA is a water-soluble polyphenol compound with a complex chemical structure ($C_{76}H_{52}O_{46}$; Fig. 1), containing a glucose core covalently linked to 3-5 gallic acid residues through the hydrolysis of ester bonds (39). TA has been revealed to exert antioxidant, anti-inflammatory, anticarcinogenic, antimutagenic and anti-atherogenic properties (40). It is also capable of protecting against drug toxicity (41).

Our previous studies have indicated that TA has beneficial effects on cardiovascular disease (42-44); moreover, we found that TA ameliorates ATO-induced nephrotoxicity (45). However, the effects of TA on ATO-induced cardiotoxicity have not yet been reported. The aim of the present study was to evaluate whether TA can protect against ATO-induced heart injury in rats.

Materials and methods

Chemicals and materials. TA (>98% purity) was acquired from Sigma-Aldrich (Merck KGaA). ATO was purchased from Beijing SL Pharmaceutical Co., Ltd. Kits for determining total CK and LDH, as well as catalase (CAT), malondialdehyde (MDA) and superoxide dismutase (SOD) activity were obtained from Nanjing Jiancheng Bioengineering Institute. All solvents were analytical grade and commercially available.

Animals and experimental protocol. A total of 50 adult male Sprague-Dawley rats (age, 6-8 weeks; weight, 180-220 g) were obtained from Hebei Medical University. Male rats were raised under standard conditions (22-25°C and 45-55% relative humidity with a 12-h light/dark cycle), with *ad libitum* access to pellet food and water. Animal experiments were performed in accordance with the Animal Care and Ethics Committee of Hebei University of Chinese Medicine (Shijiazhuang, China). The Animal Care and Ethics Committee of Hebei University of Chinese Medicine approved all animal protocols (approval no. DWLL2018038).

Male rats were stochastically separated into five groups: i) Control (Control, 0.1 ml/kg/day); ii) ATO-alone (ATO, 5 mg/kg/day); iii) ATO + low-dose TA (ATO + L-TA, 20 mg/kg/day); iv) ATO + high-dose TA (ATO + H-TA, 40 mg/kg/day); and v) TA-alone (TA, 40 mg/kg/day). Rats were intraperitoneally (i.p.) injected with ATO (5 mg/kg) to establish an ATO-induced cardiotoxicity model. Dose selection was determined according to previous literature (46,47). Studies have reported that the median lethal dose of ATO is 14.98 mg/kg body weight in rats (48,49). The Control group received isovolumic normal saline. The ATO + L-TA and ATO + H-TA groups underwent intragastric administration of TA (20 and 40 mg/kg/day, respectively) every morning and were intraperitoneally injected with ATO (5 mg/kg/day) every afternoon (40,42,45). After 7 days, sodium pentobarbital (40 mg/kg, i.p.; Sigma-Aldrich; Merck KGaA) was used to anesthetize rats, and the heart was removed and measured.

Histopathological examination. Cardiac specimens were fixed in 4% paraformaldehyde at room temperature for 48 h. Following fixation, all paraffin-embedded samples were sectioned at 4 µm and stained at room temperature with 0.1% hematoxylin (Hebei Bohai Biological Engineering Development Co., Ltd.) for 5 min and 0.5% eosin for 3 min (50). Finally, pathological changes in myocardial tissue structure were examined under a light microscope at x400 magnification (Leica DM4000B; Leica Microsystems GmbH).

Measurement of cardiac marker enzymes. Rat serum was separated by centrifugation at 1,500 x g for 10 min at 4°C
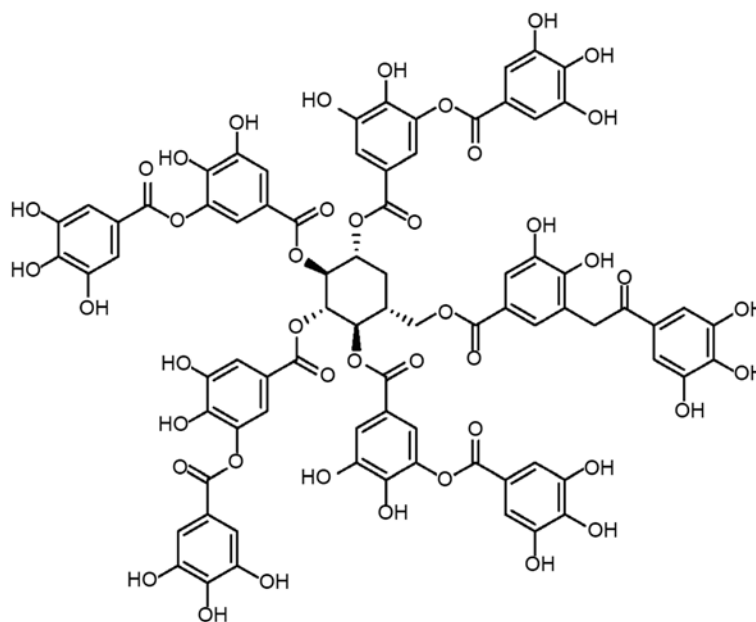
Figure 1. Structure of tannic acid.

and the activity of CK and LDH were detected using CK (cat. no. A032) and LDH (cat. no. A020-1) assay kits (both Nanjing Jiancheng Bioengineering Institute), respectively. For CK assay, serum samples (20 μl) and mixed reagent were added into tubes according to the manufacturer's protocol, then vortex mixed and incubated at 37°C for 20 min. Then, R6 solution from the kit was added and the mixed solution was centrifuged at 3,500 x g for 10 min at room temperature. Next, the tubes were heated in a water bath at 45°C for 15 min and the absorbance was detected at 660 nm using a microplate reader (Varioskan LUX; Thermo Fisher Scientific, Inc.). The activity of CK was calculated according to the formula provided in the manufacturer's protocol.

For the LDH assay, serum samples (20 μl; 1:50), buffer solution and coenzyme I solution were added into tubes, vortex mixed and incubated at 37°C for 15 min, according to the manufacturer's protocol. Then, 2,4-dinitrophenylhydrazine solution was added before being vortex mixed and incubated at 37°C for 15 min. Next, NaOH solution was added and incubated at room temperature for 3 min, and the absorbance was detected at 440 nm using a microplate reader (as aforementioned). The amount of LDH was assessed by measuring the levels of pyruvic acid.

Measurement of ROS. The fluorescent probe dihydroethidine (DHE) was used to measure the content of ROS in fresh heart tissue samples using an ROS detection kit (cat. no. KGAF019; Nanjing KeyGen Biotech Co., Ltd.). The specimens were embedded at optimum cutting temperature and flash-frozen in liquid nitrogen and sectioned (thickness, 5 μm) using a freezing microtome (Leica CM1950; Leica Microsystems GmbH). Then, 50 μM DHE solution was added, and sections were incubated at room temperature in a darkened incubator for 30 min. Next, sections were washed three times with PBS (5 min/wash). Finally, the sections were sealed using a water-soluble encapsulant and examined using a fluorescence microscope at x200 magnification (Leica DM4000B; Leica

Microsystems GmbH). The stained area of ROS was quantitatively analyzed using Image Pro Plus 6.0 software (Media Cybernetics, Inc.).

Measurement of serum levels of SOD, CAT and MDA. Rat serum was separated by centrifugation at 1,500 x g for 10 min at 4°C and the serum levels of SOD, CAT and MDA were detected using assay kits (cat. nos. A001-3, A007-1 and A003-1, respectively; all Nanjing Jiancheng Bioengineering Institute). According to the manufacturer's instruction, serum samples and relevant solutions of the SOD assay kit were mixed and incubated at 37°C for 20 min, then the absorbance was measured at 450 nm using a microplate reader (as aforementioned). The activity of SOD was calculated as U/ml. Similarly, the activity of CAT and MDA were analyzed following the manufacturer's instructions. The absorbance of CAT at 405 nm and the absorbance of MDA at 532 nm were measured using a microplate reader (as aforementioned). The activity of CAT was calculated as U/ml and the contents of MDA were calculated as nmol/ml.

Immunohistochemistry. Tissue sections were subjected to conventional dewaxing to water, rehydrated in a descending series of ethanol (100, 95, 90 and 80%), and then incubated with 3% H_2O_2 for 20 min at 37°C. Sections were incubated overnight at 4°C with primary antibodies against Bax protein (1:80; cat. no. 50599-2-Ig), cytochrome *c* (1:70; cat. no. 10993-1-AP), HtrA2 (1:80; cat. no. 15775-1-AP) and Smac (1:70; cat. no. 10434-1-AP) (all ProteinTech Group, Inc.). Next, sections were washed three times using PBS solution. The sections were incubated with horseradish peroxidase-conjugated secondary antibody (1:2,000, cat. no. PV-6001; OriGene Technologies, Inc.) for 20 min at room temperature, and then stained using the 3,3'diaminobenzidine (DAB) substrate kit (cat. no. ZLI-9019; OriGene Technologies, Inc.). Color development was induced with 0.5% DAB for 20 min at room temperature. Lastly, the heart tissue samples were re-stained

Table I. Primer sequences of p53, Bad and β-actin.

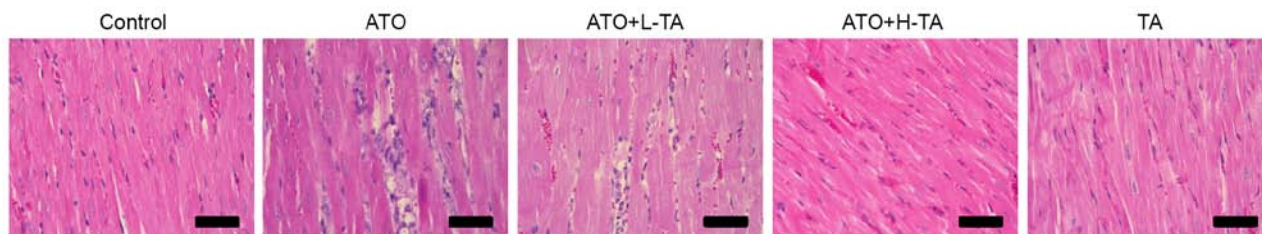| Gene	Primer sequence (5'→3')	Fragment size, bp
p53	Forward: CCCCAGGATGTTGCAGAGTTG	150
	Reverse: TTGAGAAGGGACGGAAGATGAC	
Bad	Forward: GAGTCGCCACAGTTCGTACC	156
	Reverse: TCAAATTCATCGCTCATTCTTC	
β-actin	Forward: CCTAGACTTCGAGCAAGAGA	140
	Reverse: GGAAGGAAGGCTGGAAGA	

Figure 2. Effects of TA on cardiac histopathology. Representative sections were obtained from the myocardial tissue of Control, ATO, ATO + L-TA, ATO + H-TA and TA groups. Magnification, x400; scale bar, 50 μm. TA, tannic acid; ATO, arsenic trioxide; L, low dose; H, high dose.

with 0.5% hematoxylin for 2 min at room temperature and observed under a light microscope (magnification, x400). Protein expression levels were measured using Image Pro Plus 6.0 software (Media Cybernetics, Inc.).

Western blotting. Frozen samples were weighed separately and homogenized in RIPA lysis buffer (Beijing Solarbio Science & Technology Co., Ltd.), then lysed overnight at 4˚C. The heart tissue samples were centrifuged at 12,000 x g for 10 min at 4˚C, then supernatant (total protein extract) was transferred to an EP tube and the protein level was quantified via the bicinchoninic acid method. Then, the protein samples (50 μg) were transferred onto PVDF membranes using 10% SDS-PAGE gels (EMD Millipore). The membranes were gently removed and placed in a TBST blocking buffer (5% skimmed milk in TBS-0.1% Tween-20) for 2 h at 37˚C. Next, the proteins were incubated with anti-NF-κB (p65) (1:2,000; cat. no. 10745-1-AP; ProteinTech Group, Inc.), anti-caspase 3 (1:600; cat. no. 19677-1-AP; ProteinTech Group, Inc.), anti-cleaved caspase-3 (1:800; cat. no. AF7022; Affinity Biosciences), anti-Bcl-2 (1:600; cat. no. 26593-1-AP; ProteinTech Group, Inc.) and anti-β-actin (1:1,000; cat. no. TA-09; OriGene Technologies, Inc.) overnight at 4˚C. Then, proteins were incubated with the horseradish peroxidase-labeled secondary antibody (1:3,000; cat. no. ZB-2301; OriGene Technologies, Inc.) for 90 min at room temperature. Membranes were washed three times and proteins were visualized using the ECL Detection system (TransGen Biotech Co., Ltd.). After scanning the film with a Tanon1600, the gray value of the band was measured by Tanon Gis 1D software (Tanon Science and Technology Co., Ltd.).

Reverse transcription-quantitative (RT-q)PCR. Total RNA was extracted from heart tissue samples using TRIzol (cat. no. 15596-026; Invitrogen; Thermo Fisher Scientific, Inc.). RT was performed with TIANScript RT kit (cat. no. KR104-02; Tiangen Biotech Co., Ltd.) according to the manufacturer's instructions. The gene expression levels of p53 and Bad in heart tissue were assessed via RT-qPCR using SYBR Green (cat. no. FP205; Tiangen Biotech Co., Ltd.). β-actin was used as the internal control. The PCR thermocycling conditions were: Initial denaturation (95˚C for 15 min), then 40 cycles of denaturation (95˚C for 10 sec), annealing (58˚C for 30 sec) and extension (72˚C for 30 sec). The data was analyzed with the $2^{-\Delta\Delta Cq}$ method (51). The primers used are listed in Table I.

Data analysis. Data are presented as the mean ± SEM of three independent repeats. Statistical comparisons between groups were measured using one-way ANOVA followed by Bonferroni's test. The Bonferroni correction was used as a post hoc test to eliminate false positives in multiple comparisons. Origin 7.5 (OriginLab) and SPSS 15.0 (SPSS, Inc.) statistical analysis software were used. P<0.05 was considered to indicate a statistically significant difference.

Results

Effects of TA on heart histopathology. Histological changes of rat heart samples were investigated by H&E staining. Heart tissue exhibited a normal myocardium structure and regular myocardial cell distribution in the Control group (Fig. 2). However, in the ATO group, notable myocardial tissue injury, disordered arrangement of cardiomyocytes, cell nucleus pyknosis and degeneration, increased eosinophils and focal inflammatory cell infiltration were observed. The ATO + L-TA and ATO + H-TA groups retained an almost normal myocardial tissue structure (myocardial cells arranged closely, rich cytoplasm, regular nucleus and normal cardiac muscle bundles). In addition, there was no difference in myocardial structure between the TA and Control groups.
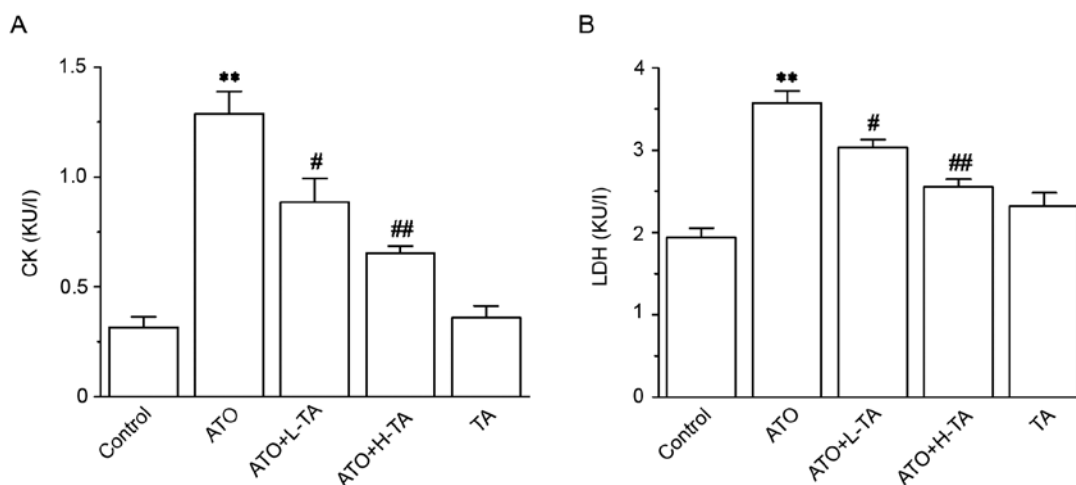
Figure 3. Effects of TA on the activity of CK and LDH. Activity of (A) CK and (B) LDH was measured in serum using commercial detection kits. Serum was collected from the Control, ATO, ATO + L-TA, ATO + H-TA, and TA groups. Data are presented as the mean ± SEM (n=6). **P<0.01 vs. Control; #P<0.05 and ##P<0.01 vs. ATO. CK, creatine kinase; LDH, lactate dehydrogenase; TA, tannic acid; ATO, arsenic trioxide; L, low dose; H, high dose.
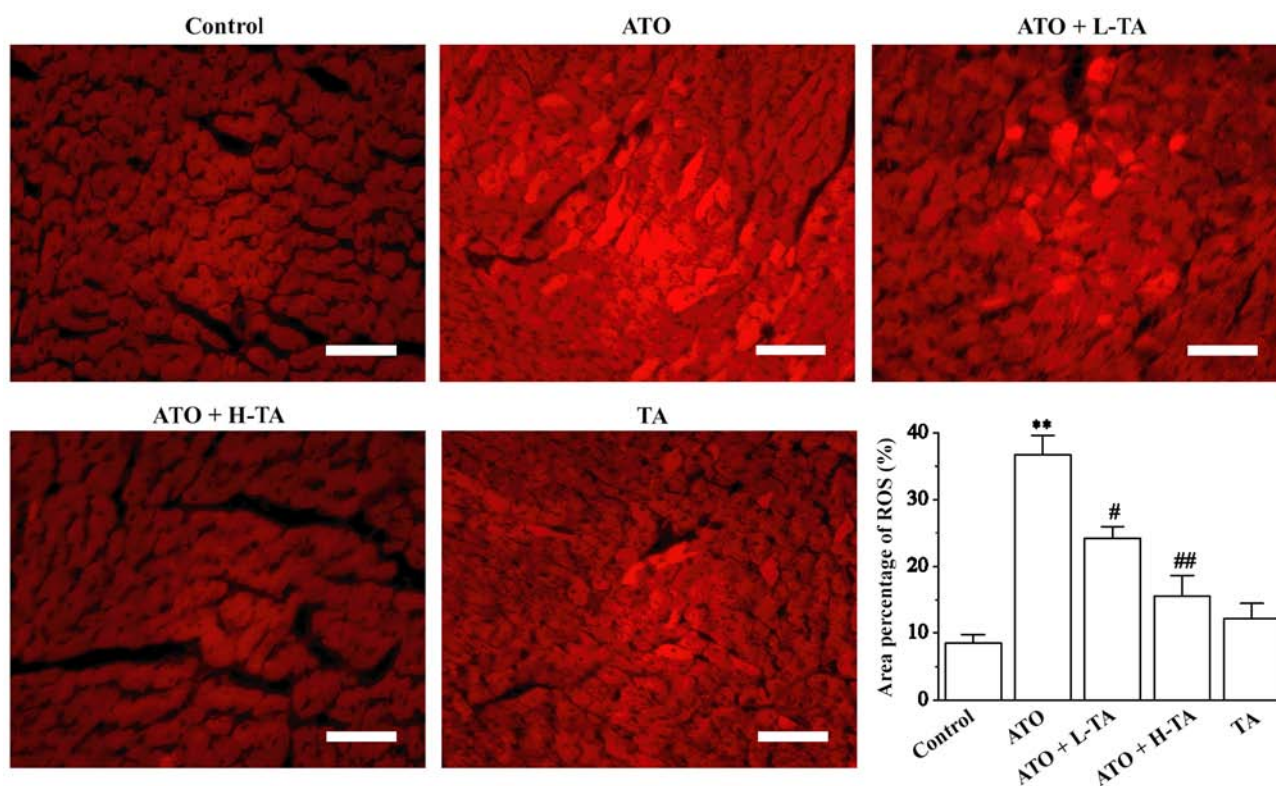

Figure 4. Effects of TA on the level of ROS in myocardial tissue. Production of ROS was measured in heart tissues with a dihydroethidium probe. The fluorescence intensity and ROS levels area percentages are shown. Magnification, x200; scale bar, 100 μm. **P<0.05 vs. Control; #P<0.05 and ##P<0.01 vs. ATO. TA, tannic acid; ROS, reactive oxygen species; ATO, arsenic trioxide; L, low dose; H, high dose.

Effects of TA on cardiotoxicity indices. CK and LDH levels in the ATO group were significantly improved compared with the Control group (Fig. 3), revealing that the experimental model was successfully established. The CK and LDH levels in the ATO + L-TA and ATO + H-TA groups were significantly decreased compared with the ATO group.

Effects of TA on oxidative stress markers. Fluorescence intensity was significantly enhanced in the ATO group, suggesting

that the level of ROS was higher in the heart tissue compared with the Control group (Fig. 4). Following TA treatment, fluorescence intensity significantly weakened. These results indicated that TA protection against ATO-induced heart damage may be associated with decreasing oxidative stress and ROS production.

Effects of TA on levels of SOD, CAT, and MDA. Serum analysis revealed that SOD (Fig. 5A) and CAT (Fig. 5B) levels in the
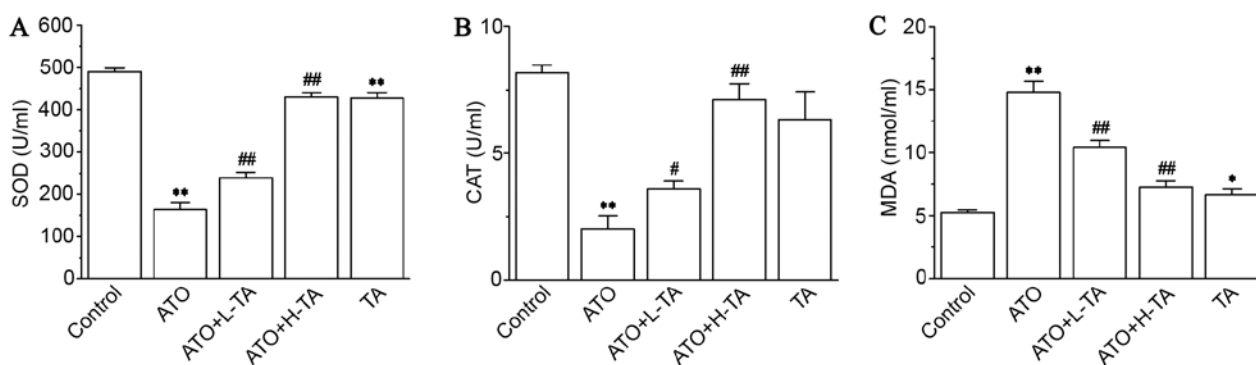
Figure 5. Effects of TA on SOD, CAT activities and MDA content in serum. Levels of (A) SOD, (B) CAT and (C) MDA were evaluated in rat heart serum using commercial detection kits. Data are presented as the mean ± SEM (n=6). *P<0.05 and **P<0.01 vs. Control; #P<0.05 and ##P<0.01 vs. ATO. TA, tannic acid; SOD, superoxide dismutase; CAT, catalase; MDA, malondialdehyde; ATO, arsenic trioxide; L, low dose; H, high dose.

ATO group were significantly decreased compared with the Control group. Compared with the ATO group, SOD and CAT activity were increased in the ATO + L-TA and ATO + H-TA groups. Moreover, MDA (Fig. 5C) levels increased following ATO exposure compared with the Control group. Following, TA administration, the levels of MDA were lower in the ATO + L-TA and ATO + H-TA groups.

Effects of TA on cytochrome c, Smac, HtrA2 and Bax expression levels. Immunohistochemistry was used to measure the expression levels of cytochrome *c*, Smac, HtrA2 and Bax in the heart tissue samples. Cytochrome *c*, Smac, HtrA2 and Bax expression levels were significantly increased in the ATO group compared with the Control (Fig. 6). Administration of 20 or 40 mg/kg/day TA decreased the expression levels of cytochrome *c*, Smac, HtrA2 and Bax, indicating that the cardiac protection of TA is a result of its anti-mitochondrial apoptosis effect.

Effects of TA on the expression levels of caspase-3, cleaved caspase-3, Bcl-2 and NF-κB (p65). Expression levels of caspase-3, cleaved caspase-3 and NF-κB (p65) were markedly increased in the ATO group (Fig. 7A and E). However, the expression levels of Bcl-2 significantly decreased (Fig. 7C). The ratio of cleaved caspase-3/caspase-3 and NF-κB (p65) was significantly upregulated in the ATO group compared with the Control (Fig. 7B and F). However, compared with the Control group, the Bcl-2 (Fig. 7D) expression levels were significantly lower in the ATO group. Following TA treatment, the ratio of cleaved caspase-3/caspase-3 was significantly decreased, and the expression levels of NF-κB (p65) were downregulated, whereas Bcl-2 expression levels were significantly increased.

Effects of TA on the expression levels of p53 and Bad. The expression levels of p53 and Bad in the ATO group were significantly increased compared with the Control group (Fig. 8). Subsequent TA administration caused a significant decrease in p53 and Bad expression levels.

Discussion

There are an increasing number of studies on the cardiotoxicity of ATO, which limits its wide clinical application (13,14). The present study established a cardiotoxicity model in rats

by intraperitoneal injection with ATO (5 mg/kg). In addition, high-dose TA-alone was administered to evaluate whether it has a toxic effect on the heart. The results demonstrated that the cardiotoxicity induced by ATO was primarily characterized by histopathological changes. In the ATO group, myocardial cells were swollen, the cytoplasm exhibited vacuolation and myocardial fiber was abnormal (swelling of myocardial fiber, interstitial oedema and myofibrillar loss. Serum increase of CK and LDH enzymes was also detected. These findings demonstrated that ATO had a toxic effect on the myocardium. Administration of TA significantly ameliorated ATO-induced pathological changes in myocardial tissue. In addition, there was no difference in myocardial structure between the TA and Control groups. Compared with the Control group, the levels of CK and LDH in the TA group were not significantly different. These results indicated that high-dose TA alone hardly induced cardiotoxicity.

Candidate mechanisms for the cardiotoxicity induced by ATO include changes of cardiac ion channels, oxidative stress injury and cardiomyocyte apoptosis (51). Compared with other cells, cardiomyocytes are more susceptible to oxidative stress due to weak antioxidant defenses (52) and enrichment of mitochondria (30).

Oxidative stress is considered to be an imbalance between generation of ROS and the activity of antioxidant defenses. Oxidative stress is a negative consequence of the *in vivo* production of radicals, and it is considered to be an important factor leading to apoptosis (34). Multiple studies have reported that high a concentration of arsenic can cause oxidative stress and increase ROS (53,54). Excessive ROS cause injury to numerous types of macromolecules, including DNA, lipid and protein (34,55). ROS alters cell signaling processes, such as gene expression level changes, transcription factor activation and apoptosis (56). ATO has a high affinity with sulfhydryl groups (57). ATO can penetrate the cell membrane and reach the cytoplasm via diffusion, resulting in cytotoxicity by increasing ROS (58). ROS are eliminated by the catalytic deactivation of SOD and CAT *in vivo*. Therefore, these enzymes can protect the body from radicals (59). In myocardial cells, the electron transport chain, situated in the internal membrane of the mitochondria, is the primary source of ROS (60). Myocardial cells provide energy essential for cellular survival and function. In addition, CK and LDH serve important roles in energy metabolism *in vivo*. CK and LDH are also important
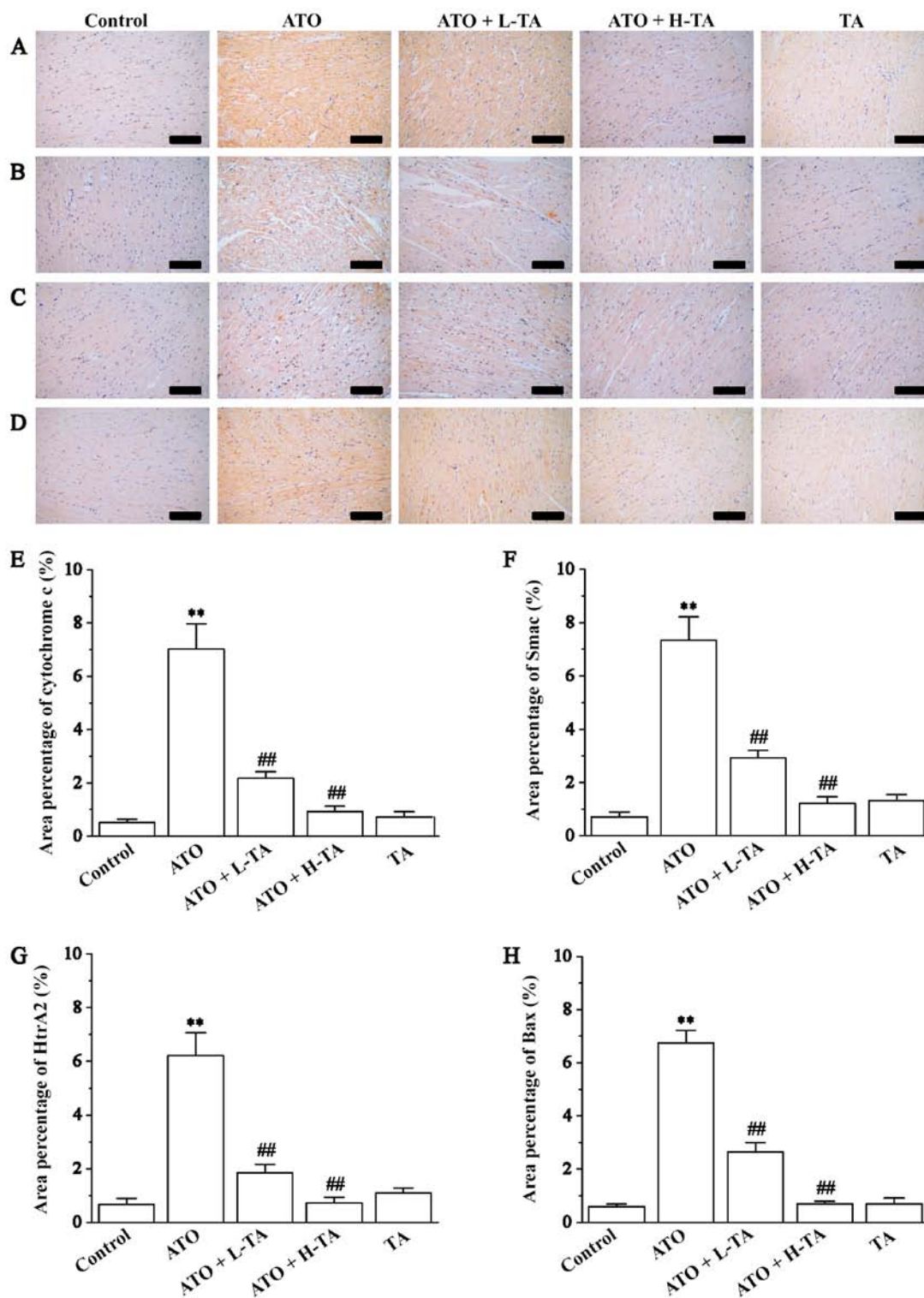
Figure 6. Effects of TA on the expression levels of cytochrome *c*, Smac, HtrA2 and Bax. Morphological orientation of the expression levels of (A) cytochrome *c*, (B) Smac, (C) HtrA2 and (D) Bax in myocardial tissue, as measured by immunohistochemistry. Magnification, x200; scale bar, 50 μm. Area percentage content of (E) cytochrome *c*, (F) Smac, (G) HtrA2 and (H) Bax was calculated in the Control, ATO, ATO + L-TA, ATO + H-TA and TA groups. Data are presented as the mean ± SEM (n=6). **$P<0.01$ vs. Control; ##$P<0.01$ vs. ATO. Smac, second mitochondria-derived activator of caspases; HtrA2, high-temperature requirement A2; TA, tannic acid; ATO, arsenic trioxide; L, low dose; H, high dose.

parameters for the diagnosis of myocardial injury (25). In the present study, following ATO administration, CAT and SOD activity markedly decreased, and the MDA levels markedly increased in serum. This result suggested that the cardiotoxicity of ATO was associated with oxidative stress injury and that TA significantly improved this phenomenon.

Mitochondria have long been considered to serve a considerable role in cell growth. However, the important function of mitochondria in programmed cell death was not recognized until the mid-1990s (61). Mitochondria are not only an important site generating cellular energy, but also the primary source of ROS and free radicals (23). Concurrently,
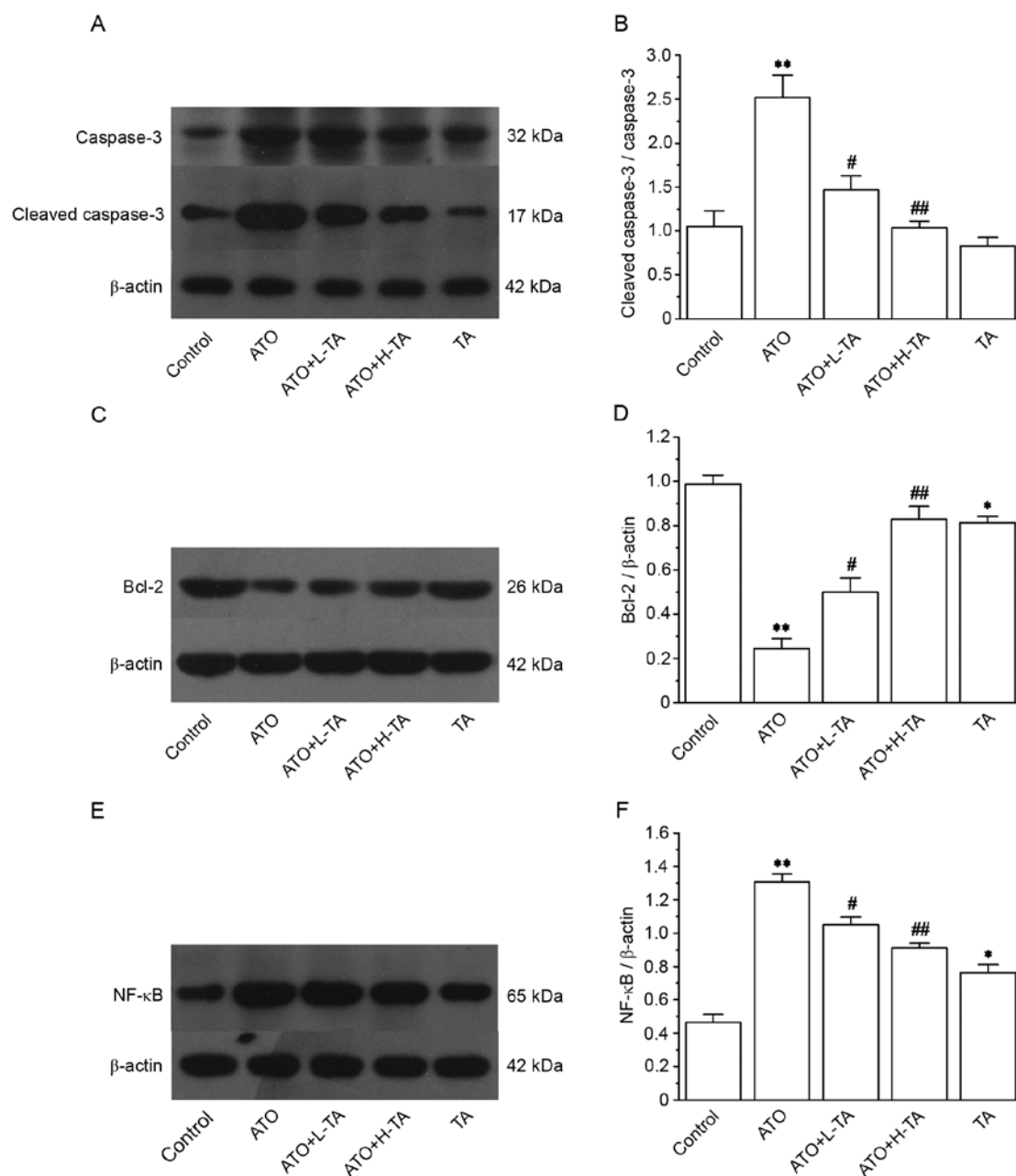
Figure 7. Effects of TA on caspase-3, cleaved caspase-3, Bcl-2 and NF-κB (p65) expression levels in rat heart. (A) Protein expression levels of caspase-3 and cleaved caspase-3 were measured by western blot analysis and (B) intensity was normalized to β-actin. (C) Protein expression levels of Bcl-2 were measured by western blot analysis and (D) intensity was normalized to β-actin. (E) Protein expression levels of NF-κB (p65) were measured by western blot analysis and (F) intensity of was normalized to β-actin. Data are presented as the mean ± SEM (n=3). *P<0.05 and **P<0.01 vs. Control; #P<0.05 and ##P<0.01 vs. ATO. TA, tannic acid; ATO, arsenic trioxide; L, low dose; H, high dose.

the mitochondria are the target of multiple apoptotic signals, which contribute to apoptosis (62). Studies have shown that polyphenols affect mitochondrial function and structure by modulating biosynthesis (mitogenesis), dynamics (fission, fusion), transport and autophagic cleavage of damaged mitochondria (mitophagy) (63,64). Wang *et al* (65) revealed that curcumin downregulated PI3K/AKT/mTOR and mTOR/p70S6K signaling pathways and activated autophagy, thus demonstrating neuroprotection in APP/presenilin 1 double transgenic mice. Apoptosis or programmed death is the mechanism of cell evolutionary conservation, which selectively removes aged, damaged and other unnecessary cells. This is a crucial part of numerous normal physiological

processes, such as embryonic development, normal tissue growth and immunoreaction (66). Apoptosis is mediated by caspase activation (67). Caspase is the effector of apoptosis; it can bind to multiple types of substrate, resulting in specific biochemical and morphological changes in apoptotic cells, including changes in mitochondrial membrane permeability, cytoskeleton reorganization, exposure of phosphatidyl-serine and DNA fragmentation (68). Endogenous apoptosis is caused by mitochondrial activation of oxidative stress. Certain mitochondrial proteins, such as pro-apoptotic factor, cytochrome *c* apoptosis-inducing factor, Smac, HtrA2 and endonuclease G, serve a regulatory role in apoptosis (63). The first released proteins are cytochrome *c*, Htr2A and Smac
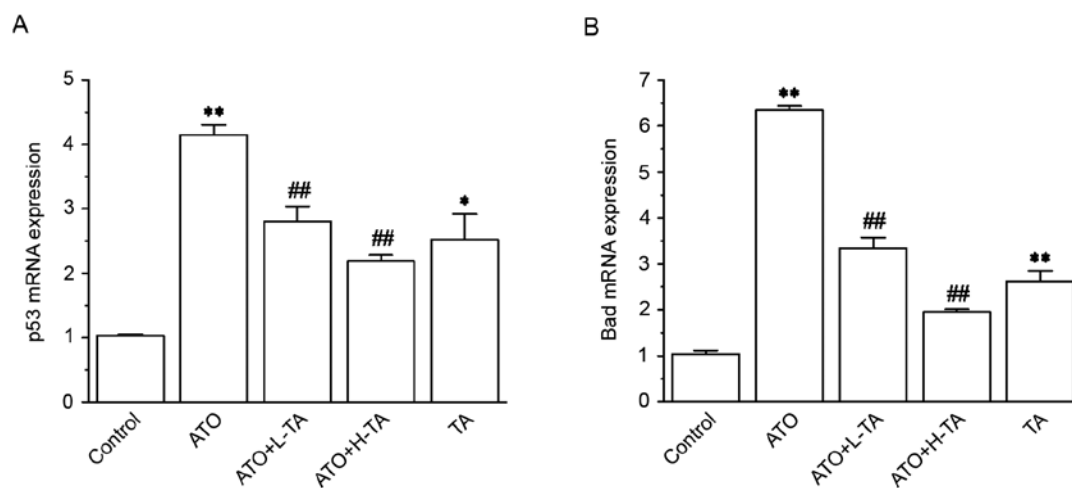
Figure 8. Effects of TA on p53 and Bad expression levels. Gene expression levels of (A) p53 and (B) Bad were examined by reverse transcription-quantitative PCR. Cardiac samples were obtained from the Control, ATO, ATO + L-TA, ATO + H-TA and TA groups. Data are presented as the mean ± SEM (n=3). *$P < 0.05$ and **$P < 0.01$ vs. Control; ##$P < 0.01$ vs. ATO. TA, tannic acid; ATO, arsenic trioxide; L, low dose; H, high dose.

in the mitochondrial apoptosis pathway, and cytochrome c, released into the cytoplasm, is combined with apoptotic protease-activating factor to form associated apoptotic bodies. This promotes the self-activation of the caspase-9 precursor, then initiates the caspase-3 precursor and cleaves caspase-3, resulting in apoptosis (69). In the present study, the ratio of cleaved caspase-3/caspase-3 was increased, which suggested activation of the caspase apoptosis pathway. Moreover, Du et al (70) revealed that Smac/DIABLO enhances cytochrome c-mediated caspase-3 activity. The present results demonstrated an increase in expression levels of cytochrome c, Smac and Htr2A, as well as the ratio of cleaved caspase-3/caspase-3, in the ATO group, confirming that ATO induced apoptotic events. The present study showed that TA treatment markedly downregulated the expression levels of the aforementioned apoptosis-associated genes and decreased the number of apoptotic cells in the ATO + L-TA and ATO + H-TA groups. In addition, the TA group exhibited no significant difference in these protein expression levels.

Bcl-2 family proteins include anti-apoptotic genes Bcl-2 and apoptosis stimulating proteins, such as Bad and Bax (71). These regulate the release of cytochrome c and the activation of caspase-3, which play an essential role in the control of mitochondrial apoptosis (72). The p53 protein is a tumor suppressor and serves a crucial role in the regulation of mitochondrial apoptosis, cell cycle and senescence (69). p53 signaling activates the transcription of Bad and Bax (73,74) and suppresses the transcription of Bcl-2 (75,76). A previous study demonstrated that low levels of p53 contribute to maintaining mitochondrial activity and function (77). Additionally, studies have reported that arsenic exposure causes the phosphorylation of the NF-κB (p65) pathway (36,78). Activation of the NF-κB pathway triggers an inflammatory response, which induces apoptosis. NF-κB exhibits pro-inflammatory properties (79), and apoptosis is an indispensable mechanism that inhibits prolonged inflammation (80). In accordance with published studies, we observed that ATO exposure increased the expression levels of p53 protein, Bax, Bad and NF-κB (p65) and decreased those of Bcl-2 in rat heart. These results

demonstrated that ATO induced myocardial apoptosis via mitochondria dysfunction and inflammation. Furthermore, following administration of TA, the expression levels of p53 protein, Bax, Bad and NF-κB (p65) were suppressed and Bcl-2 protein expression levels were promoted.

Based on the findings obtained from the present study, we hypothesize that the beneficial protective effect of TA may be achieved via ameliorating ATO-induced injury of cardiomyocytes and inhibiting the release of cardiac marker enzymes from the myocardium. In the present study, TA significantly improved ATO-induced oxidative stress injury and mitochondrial function due to ROS scavenging properties. As such, TA ameliorates ATO-induced cardiomyocyte apoptosis via decreasing the release of mitochondrial-associated proteins cytochrome c, Smac and Htr2A and inhibition of caspase-3 activation. In addition, the present study indicated that TA plays an anti-inflammatory role by inhibiting the activation of the NF-κB pathway; similarly, TA has a significant suppression of ATO-induced activation of the p53 pathway resulting in decreased release of Bax and increasing the release of Bcl-2. This protected the cardiomyocytes from ATO-induced cell death.

The present study investigated the potential effects and mechanisms of TA against ATO-induced cardiotoxicity. It has recently been reported that combination of TA and antitumor agent cisplatin may exert synergistic anticancer effects and may be a novel adjuvant treatment for liver cancer (81). Our next study will investigate whether TA has synergistic or antagonistic effects when combined with ATO to treat malignant tumors.

In conclusion, the present data suggested that mitochondrial dysfunction contributed to the cardiotoxicity of ATO, as well as to an oxidative stress reaction and inflammatory response. The present study demonstrated that TA administration effectively improved ATO-induced cardiotoxicity. The protective functions of TA may be associated with suppression of activation of the mitochondrial apoptosis pathway. Collectively, the present findings revealed that TA provided effective protection against ATO-induced cardiotoxicity.

Based on these results, TA may have a potential defense mechanism in ATO clinical therapy and diminish its cardiotoxic effects. However, further investigation is required before its clinical application.

Availability of data and materials

The datasets used and/or analyzed during the current study are available from the corresponding author on reasonable request.

Authors' contributions

YucX, ML, XC and LC conceived and designed the study. YucX, ML, YurX, WJ and XH performed the experiments. YucX and LC contributed to the writing of the original draft. ML contributed to data collection and interpretation. YurX and WJ provided help for analyzing the data. XH and JZ supervised the experiments and interpreted data. XC and ZL provided guidance for software and figures. YucX, ZL and LC revised the manuscript. All authors read and approved the final manuscript.

Ethics approval and consent to participate

Animal experiments were performed at Hebei Medical University of Chinese Medicine were in accordance with the Animal Care and Ethics Committee of Hebei Medical University of Chinese Medicine (Shijiazhuang, China) under the provisions of the UK Animals (Scientific Procedures) Act 1986. The Animal Care and Ethics Committee of Hebei Medical University of Chinese Medicine approved all animal protocols (approval no. DWLL2018038).

Patient consent for publication

Not applicable.

Competing interests

The authors declare that they have no competing interests.

References

1. Alamolhodaei NS, Shirani K and Karimi G: Arsenic cardiotoxicity: An overview. Environ Toxicol Pharmacol 40: 1005-1014, 2015.
2. Manna P, Sinha M and Sil PC: Arsenic-induced oxidative myocardial injury: Protective role of arjunolic acid. Arch Toxicol 82: 137-149, 2008.
3. Mathews V, Chendamarai E, George B, Viswabandya A and Srivastava A: Treatment of acute promyelocytic leukemia with single-agent arsenic trioxide. Mediterr J Hematol Infect 3: e2011056, 2011.
4. Zhang TC, Cao EH, Li JF, Ma W and Qin JF: Induction of apoptosis and inhibition of human gastric cancer MGC-803 cell growth by arsenic trioxide. Eur J Cancer 35: 1258-1263, 1999.
5. Shen ZY, Zhang Y, Chen JY, Chen MH, Shen J, Luo WH and Zeng Y: Intratumoral injection of arsenic to enhance antitumor efficacy in human esophageal carcinoma cell xenografts. Oncol Rep 11: 155-159, 2004.
6. Akao Y, Nakagawa Y and Akiyama K: Arsenic trioxide induces apoptosis in neuroblastoma cell lines through the activation of caspase 3 in vitro. FEBS Lett 455: 59-62, 1999.
7. Tai S, Xu LF, Xu M, Zhang LG, Zhang YY, Zhang KP, Zhang L and Liang CZ: Combination of arsenic trioxide and everolimus (Rad001) synergistically induces both autophagy and apoptosis in prostate cancer cells. Oncotarget 8: 11206-11218, 2017.
8. Bao ZY, Han ZB, Zhang B, Yu Y, Xu ZH, Ma WY, Ding FZ, Zhang L, Yu MX, Liu SZ, *et al*: Arsenic trioxide blocked proliferation and cardiomyocyte differentiation of human induced pluripotent stem cells: Implication in cardiac developmental toxicity. Toxicol Lett 309: 51-58, 2019.
9. Liu YS, Liang YR, Zheng B, Chu L, Ma DL, Wang HF, Chu X and Zhang JP: Protective Effects of crocetin on arsenic trioxide-induced hepatic injury: Involvement of suppression in oxidative stress and inflammation through activation of Nrf2 signaling pathway in rats. Drug Des Devel Ther 14: 1921-1931, 2020.
10. Unnikrishnan D, Dutcher JP, Garl S, Varshneya N, Lucariello R and Wiernik PH: Cardiac monitoring of patients receiving arsenic trioxide therapy. Br J Haematol 124: 610-617, 2004.
11. Mu MY, Zhao HJ, Wang Y, Liu JJ, Fei DX and Xing MW: Arsenic trioxide or/and copper sulfate co-exposure induce glandular stomach of chicken injury via destruction of the mitochondrial dynamics and activation of apoptosis as well as autophagy. Ecotoxicol Environ Saf 185: 109678, 2019.
12. Badarkhe GV, Sil A, Bhattacharya S, Nath UK and Das NK: Erythema multiforme due to arsenic trioxide in a case of acute promyelocytic leukemia: A diagnostic challenge. Indian J Pharmacol 48: 216-218, 2016.
13. Roboz GJ, Ritchie EK, Carlin RF, Samuel M, Gale L, Provenzano-Gober JL, Curcio TJ, Feldman EJ and Kligfield PD: Prevalence, management, and clinical consequences of QT interval prolongation during treatment with arsenic trioxide. J Clin Oncol 32: 3723-3728, 2014.
14. Hai JJ, Gill H, Tse HF, Kumana CR, Kwong YL and Siu CW: Torsade de pointes during oral arsenic trioxide therapy for acute promyelocytic leukemia in a patient with heart failure. Ann Hematol 94: 501-503, 2015.
15. Zhang Y, Wei ZK, Liu WJ, Wang JJ, He XX, Huang HL, Zhang JL and Yang ZT: Melatonin protects against arsenic trioxide-induced liver injury by the upregulation of Nrf2 expression through the activation of PI3K/AKT pathway. Oncotarget 8: 3773-3780, 2017.
16. Wang XN, Zhao HY, Shao YL, Wang P, Wei YR, Zhang WQ, Jiang J, Chen Y and Zhang Z: Nephroprotective effect of astaxanthin against trivalent inorganic arsenic-induced renal injury in wistar rats. Nutr Res Pract 8: 46-53, 2014.
17. Cheng Y, Xue J, Jiang H, Wang M, Gao L, Ma D and Zhang Z: Neuroprotective effect of resveratrol on arsenic trioxide-induced oxidative stress in feline brain. Hum Exp Toxicol 33: 737-747, 2014.
18. Ahamed M, Akhtar MJ and Alhadlaq HA: Co-exposure to SiO_2 nanoparticles and arsenic induced augmentation of oxidative stress and mitochondria-dependent apoptosis in human cells. Int J Environ Res Public Health 16: 3199, 2019.
19. Sabbah HN: Targeting the mitochondria in heart failure: A translational perspective. JACC Basic Transl Sci 5: 88-106, 2020.
20. Chistiakov DA, Shkurat TP, Melnichenko AA, Grechko AV and Orekhov AN: The role of mitochondrial dysfunction in cardiovascular disease: A brief review. Ann Med 50: 121-127, 2018.
21. Roy D, Felty Q, Narayan S and Jayakar P: Signature of mitochondria of steroidal hormones-dependent normal and cancer cells: Potential molecular targets for cancer therapy. Front Biosci 12: 154-173, 2007.
22. Brown DA, Perry JB, Allen ME, Sabbah HN, Stauffer BL, Shaikh SR, Cleland JG, Colucci WS, Butler J, Voors AA, *et al*: Expert consensus document: Mitochondrial function as a therapeutic target in heart failure. Nat Rev Cardiol 14: 238-250, 2017.
23. Pohjoismäki JL and Goffart S: The role of mitochondria in cardiac development and protection. Free Radic Biol Med 106: 345-354, 2017.

24. Peoples JN, Saraf A, Ghazal N, Pham TT and Kwong JQ: Mitochondrial dysfunction and oxidative stress in heart disease. Exp Mol Med 51: 1-13, 2019.
25. Abdelrahman RS, El-Awady MS, Nader MA and Ammar EM: Hydrogen sulfide ameliorates cardiovascular dysfunction induced by cecal ligation and puncture in rats. Hum Exp Toxicol 34: 953-964, 2015.
26. Gill C, Mestril R and Samali A: Losing heart: The role of apoptosis in heart disease-a novel therapeutic target? FASEB J 16: 135-146, 2002.
27. Yu XJ, Wang ZY, Shu ZP, Li ZQ, Ning Y, Yun KL, Bai HN, Liu RH and Liu WL: Effect and mechanism of Sorbus pohuashanensis (Hante) Hedl. Flavonoids protect against arsenic trioxide-induced cardiotoxicity. Biomed Pharmacother 88: 1-10, 2017.
28. McDonough KH: The role of alcohol in the oxidant antioxidant balance in heart. Front Biosci 4: D601-D606, 1999.
29. Wang Y, Wu YP, Wang YY, Xu H, Mei XQ, Yu DY, Wang YB and Li WF: Antioxidant properties of probiotic bacteria. Nutrients 9: 521, 2017.
30. Vineetha VP, Soumya RS and Raghu KG: Phloretin ameliorates arsenic trioxide induced mitochondrial dysfunction in H9c2 cardiomyoblasts mediated via alterations in membrane permeability and ETC complexes. Eur J Pharmacol 754: 162-172, 2015.
31. Lindskog M, Gleissman H, Ponthan F, Castro J, Kogner P and Johnsen JI: Neuroblastoma cell death in response to docosahexaenoic acid: Sensitization to chemotherapy and arsenic-induced oxidative stress. Int J Cancer 118: 2584-2593, 2006.
32. Chen H, Liu G, Qiao N, Kang Z, Hu L, Liao J, Yang F, Pang C, Liu B, Zeng Q, et al: Toxic effects of arsenic trioxide on spermatogonia are associated with oxidative stress, mitochondrial dysfunction, autophagy and metabolomic alterations. Ecotoxicol Environ Saf 190: 110063, 2020.
33. Patlolla AK and Tchounwou PB: Serum acetyl cholinesterase as a biomarker of arsenic induced neurotoxicity in sprague-dawley rats. Int J Environ Res Public Health 2: 80-83, 2005.
34. Vineetha VP and Raghu KG: An overview on arsenic trioxide-induced cardiotoxicity. Cardiovasc Toxicol 19: 105-119, 2019.
35. Amini-Khoei H, Hosseini MJ, Momeny M, Rahimi-Balaei M, Amiri S, Haj-Mirzaian A, Khedri M, Jahanabadi S, Mohammadi-Asl A, Mehr SE and Dehpour AR: Morphine attenuated the cytotoxicity induced by arsenic trioxide in H9c2 cardiomyocytes. Biol Trace Elem Res 173: 132-139, 2016.
36. Ghosh J, Das J, Manna P and Sil PC: Taurine prevents arsenic-induced cardiac oxidative stress and apoptotic damage: Role of NF-kappa B, p38 and JNK MAPK pathway. Toxicol Appl Pharmacol 240: 73-87, 2009.
37. Zhang JY, Sun GB, Luo Y, Wang M, Wang W, Du YY, Yu YL and Sun XB: Salvianolic acid a protects H9c2 cells from arsenic trioxide-induced injury via inhibition of the MAPK signaling pathway. Cell Physiol Biochem 41: 1957-1969, 2017.
38. Zhu S, Wang Y, Liu H, Wei W, Tu Y, Chen C, Song J, Xu Z, Li J, Wang C and Sun S: Thyroxine affects lipopolysaccharide-induced macrophage differentiation and myocardial cell apoptosis via the NF-κB p65 pathway both in vitro and in vivo. Mediators Inflamm 2019: 2098972, 2019.
39. Liu X, Kim J, Li Y, Li J, Liu F and Chen X: Tannic acid stimulates glucose transport and inhibits adipocyte differentiation in 3T3-L1 cells. J Nutr 135: 165-171, 2005.
40. Hemmati AA, Olapour S, Varzi HN, Khodayar MJ, Dianat M, Mohammadian B and Yaghooti H: Ellagic acid protects against arsenic trioxide-induced cardiotoxicity in rat. Hum Exp Toxicol 37: 412-419, 2018.
41. Ashafaq M, Sharma P, Khatoon S, Haque D, Tabassum H and Parvez S: Heavy metal-induced systemic dysfunction attenuated by tannic acid. J Environ Pathol Toxicol Oncol 35: 109-120, 2016.
42. Zhang JP, Cui LJ, Han X, Zhang YY, Zhang X, Chu X, Zhang FH, Zhang Y and Chu L: Protective effects of tannic acid on acute doxorubicin-induced cardiotoxicity: Involvement of suppression in oxidative stress, inflammation, and apoptosis. Biomed Pharmacother 93: 1253-1260, 2017.
43. Chu L, Li PY, Song T, Han X, Zhang X, Song QT, Liu T, Zhang YY and Zhang JP: Protective effects of tannic acid on pressure overload-induced cardiac hypertrophy and underlying mechanisms in rats. J Pharm Pharmacol 69: 1191-1207, 2017.
44. Zhu FL, Chu X, Wang H, Zhang X, Zhang YY, Liu ZY, Guo H, Liu HY, Liu Y, Chu L and Zhang JP: New Findings on the effects of tannic acid: Inhibition of L-Type calcium channels, Calcium transient and contractility in rat ventricular myocytes. Phytother Res 30: 510-516, 2016.
45. Jin WY, Xue YR, Xue YC, Han X, Song QT, Zhang JP, Li ZL, Cheng J, Guan SJ, Sun SJ and Chu L: Tannic acid ameliorates arsenic trioxide-induced nephrotoxicity, contribution of NF-κB and Nrf2 pathways. Biomed Pharmacother 126: 110047, 2020.
46. Kumazaki M, Ando H, Sasaki A, Koshimizu TA, Ushijima K, Hosohata K, Oshima Y and Fujimura A: Protective effect of α-lipoic acid against arsenic trioxide-induced acute cardiac toxicity in rats. J Pharmacol Sci 115: 244-248, 2011.
47. Miao X, Tang ZF, Wang YG, Su GF, Sun WX, Wei W, Li W, Miao LN, Cai L, Tan Y and Liu QJ: Metallothionein prevention of arsenic trioxide-induced cardiac cell death is associated with its inhibition of mitogen-activated protein kinases activation in vitro and in vivo. Toxicol Lett 220: 277-285, 2013.
48. Saxena PN, Anand S, Saxena N and Bajaj P: Effect of arsenic trioxide on renal functions and its modulation by curcuma aromatica leaf extract in albino rat. J Environ Biol 30: 527-531, 2009.
49. Liu J, Lu Y, Wu Q, Goyer RA and Waalkes MP: Mineral arsenicals in traditional medicines: Orpiment, realgar, and arsenolite. J Pharmacol Exp Ther 326: 363-368, 2008.
50. Song J, Ding WB, Liu BJ, Liu D, Xia Z, Zhang L, Cui L, Luo Y, Jia XB and Feng L: Anticancer effect of caudatin in diethylnitrosamine-induced hepatocarcinogenesis in rats. Mol Med Rep 22: 697-706, 2020.
51. Livak KJ and Schmittgen TD: Analysis of relative gene expression data using real-time quantitative PCR and the 2(-Delta Delta C(T)) method. Methods 25: 402-408, 2001.
52. Costa VM, Carvalho F, Duarte JA, Bastos Mde L and Remiao F: The heart as a target for xenobiotic toxicity: The cardiac susceptibility to oxidative stress. Chem Res Toxicol 26: 1285-1311, 2013.
53. James TN: Long reflections on the QT interval: The sixth annual Gordon K. Moe Lecture. J Cardiovasc Electrophysiol 7: 738-759, 1996.
54. Best PJ, Hasdai D, Sangiorgi G, Schwartz RS, Holmes DR Jr, Simari RD and Lerman A: Apoptosis. Basic concepts and implications in coronary artery disease. Arterioscler Thromb Vasc Biol 19: 14-22, 1999.
55. Matsui M, Nishigori C, Toyokuni S, Takada J, Akaboshi M, Ishikawa M, Imamura S and Miyachi Y: The role of oxidative DNA damage in human arsenic carcinogenesis: Detection of 8-hydroxy-2'-deoxyguanosine in arsenic-related Bowen's disease. J Invest Dermatol 113: 26-31, 1999.
56. Berridge MJ, Lipp P and Bootman MD: The versatility and universality of calcium signalling. Nat Rev Mol Cell Biol 1: 11-21, 2000.
57. Pulido MD and Parrish AR: Metal-induced apoptosis: Mechanisms. Mutat Res 533: 227-241, 2003.
58. Torka P, Al Ustwani O, Wetzler M, Wang ES and Griffiths EA: Swallowing a bitter pill-oral arsenic trioxide for acute promyelocytic leukemia. Blood Rev 30: 201-211, 2016.
59. Sugden PH and Clerk A: Oxidative stress and growth-regulating intracellular signaling pathways in cardiac myocytes. Antioxid Redox Signal 8: 2111-2124, 2006.
60. Vineetha RC, Binu P, Arathi P and Nair RH: L-ascorbic acid and alpha-tocopherol attenuate arsenic trioxide-induced toxicity in H9c2 cardiomyocytes by the activation of Nrf2 and Bcl2 transcription factors. Toxicol Mech Methods 28: 353-360, 2018.
61. Petit PX, Susin SA, Zamzami N, Mignotte B and Kroemer G: Mitochondria and programmed cell death: Back to the future. FEBS Lett 396: 7-13, 1996.
62. Lopez J and Tait SW: Mitochondrial apoptosis: Killing cancer using the enemy within. Br J Cancer 112: 957-962, 2015.
63. Naoi M, Wu Y, Shamoto-Nagai M and Maruyama W: Mitochondria in neuroprotection by phytochemicals: Bioactive polyphenols modulate mitochondrial apoptosis system, function and structure. Int J Mol Sci 20: 2451, 2019.
64. Teixeira J, Deus CM, Borges F and Oliveira PJ: Mitochondria: Targeting mitochondrial reactive oxygen species with mitochondriotropic polyphenolic-based antioxidants. Int J Biochem Cell Biol 97: 98-103, 2018.
65. Wang C, Zhang X, Teng ZP, Zhang T and Li Y: Downregulation of PI3K/Akt/mTOR signaling pathway in curcumin-induced autophagy in APP/PS1 double transgenic mice. Eur J Pharmacol 740: 312-320, 2014.

66. Tower J: Programmed cell death in aging. Ageing Res Rev 23: 90-100, 2015.
67. Moloudi K, Neshasteriz A, Hosseini A, Eyvazzadeh N, Shomali M, Eynali S, Mirzaei E and Azarnezhad A: Synergistic Effects of arsenic trioxide and radiation: Triggering the intrinsic pathway of apoptosis. Iran Biomed J 21: 330-337, 2017.
68. Adil M, Kandhare AD, Ghosh P and Bodhankar SL: Sodium arsenite-induced myocardial bruise in rats: Ameliorative effect of naringin via TGF-β/Smad and Nrf/HO pathways. Chem Biol Interact 253: 66-77, 2016.
69. Estaquier J, Vallette F, Vayssiere JL and Mignotte B: The mitochondrial pathways of apoptosis. Adv Exp Med Biol 942: 157-183, 2012.
70. Du CY, Fang M, Li YC, Lily L and Wang XD: Smac, a mitochondrial protein that promotes cytochrome c-dependent caspase activation by eliminating IAP inhibition. Cell 102: 33-42, 2000.
71. Boise LH, Gottschalk AR, Quintáns J and Thompson CB: Bcl-2 and Bcl-2-related proteins in apoptosis regulation. Curr Top Microbiol Immunol 200: 107-121, 1995.
72. Tischner D, Woess C, Ottina E and Villunger A: Bcl-2-regulated cell death signalling in the prevention of autoimmunity. Cell Death Dis 1: e48, 2010.
73. Miyashita T and Reed JC: Tumor suppressor p53 is a direct transcriptional activator of the human bax gene. Cell 80: 293-299, 1995.
74. Oda E, Ohki R, Murasawa H, Nemoto J, Shibue T, Yamashita T, Tokino T, Taniguchi T and Tanaka N: Noxa, a BH3-only member of the Bcl-2 family and candidate mediator of p53-induced apoptosis. Science 288: 1053-1058, 2000.
75. Shen Y and Shenk T: Relief of p53-mediated transcriptional repression by the adenovirus E1B 19-kDa protein or the cellular Bcl-2 protein. Proc Natl Acad Sci USA 91: 8940-8944, 1994.
76. Hoffman WH, Biade S, Zilfou JT, Chen J and Murphy M: Transcriptional repression of the anti-apoptotic survivin gene by wild type p53. J Biol Chem 277: 3247-3257, 2002.
77. Bensaad K and Vousden KH: p53: New roles in metabolism. Trends Cell Biol 17: 286-291, 2007.
78. Mathas S, Lietz A, Janz M, Hinz M, Jundt F, Scheidereit C, Bommert K and Dorken B: Inhibition of NF-kappaB essentially contributes to arsenic-induced apoptosis. Blood 102: 1028-1034, 2003.
79. Pahl HL: Activators and target genes of Rel/NF-kappaB transcription factors. Oncogene 18: 6853-6866, 1999.
80. Pace C, Dagda R and Angermann J: Antioxidants protect against arsenic induced mitochondrial cardio-toxicity. Toxics 5: 38, 2017.
81. Geng NN, Zheng X, Wu MS, Yang L, Li XY and Chen JD: Tannic acid synergistically enhances the anticancer efficacy of cisplatin on liver cancer cells through mitochondria-mediated apoptosis. Oncol Rep 42: 2108-2116, 2019.